

MOL #65508

Cellular and Pharmacological Selectivity of the PPAR β/δ Antagonist GSK3787

Prajakta S. Palkar, Michael G. Borland, Simone Naruhn, Christina H. Ferry, Christina Lee, Ugir H. Sk, Arun K. Sharma, Shantu Amin, Iain A. Murray, Cherie R. Anderson, Gary H. Perdew, Frank J. Gonzalez, Rolf Müller, and Jeffrey M. Peters

Department of Veterinary and Biomedical Sciences and The Center for Molecular Toxicology and Carcinogenesis, The Pennsylvania State University, University Park, PA (P.S.P., M.G.B., C.H.F., C.L., I.A.M., C.R.A., G.H.P., J.M.P.); Institute of Molecular Biology and Tumor Research, Philipps University, Marburg, Germany (S.N., R.M.); Department of Pharmacology, Penn State Hershey Cancer Institute, The Pennsylvania State University, Milton S. Hershey Medical Center, Hershey, Pennsylvania (A.K.S., U.H.S., S.A.); Laboratory of Metabolism, National Cancer Institute, Bethesda, Maryland (F.J.G)

MOL #65508

Running title: Bioavailable PPAR β/δ antagonist

Address correspondence to: Dr. Jeffrey M. Peters, Department of Veterinary and Biomedical Sciences and The Center for Molecular Toxicology and Carcinogenesis, The Pennsylvania State University, University Park, PA 16802. Email: jmp21@psu.edu

Text Pages: 43

Tables: 1

Figures: 9 + 2 Supplemental

References: 35

Abstract : 239

Introduction: 512

Discussion: 1648

ABBREVIATIONS: Adrp, adipocyte differentiation-related protein; ANOVA, analysis of variance; Angptl4, angiopoietin-like protein 4; ChIP, chromatin immunoprecipitation; DMSO, dimethyl sulfoxide; DMEM, Dulbecco's Minimal Essential Medium; FCS, fetal calf serum; GAPDH, glyceraldehyde 3-phosphate dehydrogenase; LDH, lactate dehydrogenase; PCR, polymerase chain reaction; PPAR, peroxisome proliferator-activated receptor; PBS, phosphate buffered saline.

ABSTRACT

The availability of high affinity agonists for peroxisome proliferator-activated receptor- β/δ (PPAR β/δ) has led to significant advances in our understanding of the functional role of PPAR β/δ . In this study, a new PPAR β/δ antagonist, GSK3787, was characterized using in vivo and in vitro models. Orally administrated GSK3787 caused antagonism of GW0742-induced up-regulation of *Angptl4* and *Adrp* mRNA expression in wild-type mouse colon, but not in *Ppar β/δ* -null mouse colon. Chromatin immunoprecipitation (ChIP) analysis indicates that this correlated with reduced promoter occupancy of PPAR β/δ on the *Angptl4* and *Adrp* genes. Reporter assays demonstrated antagonism of PPAR β/δ activity, and weak antagonism and agonism of PPAR γ activity, but no effect on PPAR α activity. Time resolved fluorescence resonance energy transfer assays confirmed the ability of GSK3787 to modulate association of both PPAR β/δ and PPAR γ co-regulator peptides in response to ligand activation, consistent with reporter assays. In vivo and in vitro analysis indicates that the efficacy of GSK3787 to modulate PPAR γ activity is markedly lower than the efficacy of GSK3787 to act as a PPAR β/δ antagonist. GSK3787 antagonized GW0742-induced expression of *Angptl4* in mouse fibroblasts, mouse keratinocytes, and human cancer cell lines. Cell proliferation was unchanged in response to either GW0742 or GSK3787 in human cancer cell lines. Results from these studies demonstrate that GSK3787 can antagonize PPAR β/δ in vivo thus providing a new strategy to delineate the functional role of a receptor with great potential as a therapeutic target for the treatment and prevention of disease.

Introduction

There is considerable interest in targeting nuclear receptors for the treatment and prevention of diseases due to their ability to specifically modulate transcription of regulatory pathways that influence the etiology of diseases ranging from metabolic syndrome to cancer. This is due in part to the successful development and application of nuclear receptor agonists as therapeutic drugs. For example, the fibrate class of hypolipidemic drugs activate peroxisome proliferator-activated receptor- α (PPAR α) causing up-regulation of target genes that increase fatty acid catabolism causing decreased serum lipids and increased insulin sensitivity (Staels et al., 1998). Similarly, rosiglitazone (Avandia) and pioglitazone (Actos) both activate PPAR γ and effectively enhance insulin sensitivity and decrease serum glucose, which is the basis for their use in the treatment of type II diabetes (Gross and Staels, 2007). There is evidence supporting the development of PPAR β/δ agonists for the treatment of metabolic syndrome, diabetes and obesity, since activating PPAR β/δ increases fatty acid catabolism, ameliorates insulin resistance and decreases serum glucose (Billin, 2008). However, targeting PPAR β/δ has been met with significant issues related to clinical safety due to controversial reports surrounding the role of PPAR β/δ in cancer, with some suggesting that activating PPAR β/δ potentiates tumorigenesis while others suggest that activating PPAR β/δ attenuates tumorigenesis or has no effect (Peters and Gonzalez, 2009; Peters et al., 2008).

A number of tools have been developed in the last ten years that have significantly advanced our understanding of the role of PPAR β/δ , in particular the generation of *Ppar* β/δ -null mouse models (Barak et al., 2002; Nadra et al., 2006; Peters

MOL #65508

et al., 2000) and high affinity ligands that are more selective for PPAR β/δ (Shearer and Hoekstra, 2003). Coupling null mouse models with high affinity ligands is an excellent approach for delineating the biological function of PPAR β/δ , but there are considerable differences in responses in the different models found reported in the literature. Thus, there is a distinct need to develop alternative approaches to begin to address many of the reported disparities. Towards this goal, the recent identification of GSK0660 and SR13904 as PPAR β/δ antagonists was a step in the right direction (Shearer et al., 2008; Zaveri et al., 2009). Unfortunately, these antagonists have limited application since GSK0660 is not bioavailable and the bioavailability of SR13904 has not been evaluated (Shearer et al., 2008; Zaveri et al., 2009). In contrast, the recently described PPAR β/δ antagonist GSK3787 (Fig. 1) exhibited more suitable pharmacokinetic properties as a maximal concentration (C_{max}) of $2.2 \pm 0.4 \mu\text{M}$ with a half-life of 2.5 ± 1.1 h was attainable in mouse serum after oral administration (10 mg/kg) (Shearer et al., 2010). Moreover, GSK3787 is an irreversible antagonist of PPAR β/δ because it forms a covalent bond with a cysteine residue in the ligand binding domain of PPAR β/δ (Shearer et al., 2010). The present study provides further characterization of this new PPAR β/δ antagonist by assessing the ability of GSK3787 to antagonize PPAR β/δ function in vivo, examining the specificity of GSK3787 to antagonize PPAR β/δ using null mouse models, and by determining the effect of GSK3787 on PPAR β/δ function and cell growth in a panel of human cancer cell lines.

Materials and Methods

Materials. GW0742 (Sznaidman et al., 2003), GSK0660 (Shearer et al., 2008) and GSK3787 (Shearer et al., 2010) were synthesized by GlaxoSmithKline (Research Triangle Park, NC). GW501516, GW1929, GW7647 were purchased from Sigma-Aldrich (Steinheim, Germany). Rosiglitazone was purchased from Biomol International (Plymouth Meeting, PA).

Animals and treatments. Animal experiments were approved by the Institutional Animal Care and Use Committee at Pennsylvania State University, which conforms to the Guide for the Care and Use of Laboratory Animals published by the National Institutes of Health. For RNA and DNA analysis, male wild-type and *Ppar β / δ* -null mice (Peters et al., 2000) were administered vehicle (corn oil), GW0742 (10 mg/kg), GSK3787 (10 mg/kg), or GW0742 and GSK3787 by oral gavage 3 h prior to euthanasia. After euthanasia, colons were carefully dissected. To isolate colon epithelium, colons were flushed with phosphate buffered saline (PBS) and epithelial cells were scraped from mucosa using a razor blade. The isolated tissues were used for RNA isolation. For glucose tolerance tests, male wild-type and *Ppar β / δ* -null mice were administered vehicle (corn oil), GW0742 (10 mg/kg), GSK3787 (10 mg/kg) or rosiglitazone (20 mg/kg) by oral gavage 1X/day for 2 weeks.

RNA analysis. Colon samples were immediately homogenized in TRIzol Reagent (Invitrogen, Carlsbad, CA), and total RNA was prepared according to the

MOL #65508

manufacturer's recommended protocol. The mRNA encoding *angiopoietin-like protein 4* (*Angptl4*), *adipose differentiation-related protein* (*Adrp*), and *glyceraldehyde 3-phosphate dehydrogenase* (*Gapdh*) was measured by quantitative real-time polymerase chain reaction (qPCR) analysis. cDNA was generated from 2.5 µg of total RNA using a MultiScribe Reverse Transcriptase kit (Applied Biosystems, Foster City, CA). The real-time primers for *Angptl4*, *Adrp*, and *Gapdh* have been previously described (Hollingshead et al., 2008). qPCR reactions were carried out using SYBR green PCR master mix (Quanta BioSciences, Gaithersburg, MD) in the iCycler and detected using the MyiQ Real-Time PCR Detection System (Bio-Rad Laboratories, Hercules, CA). The following reaction conditions were used for PCR: 95°C for 15 s, 60°C for 30 s, 72°C for 30 s, repeated for 45 cycles. Each PCR included a no template reaction to control for contamination, and all PCR reactions had greater than 85% efficiency. The relative mRNA value for each gene was normalized to the relative mRNA value for *Gapdh* and analyzed for statistical significance using a two-way analysis of variance with Bonferroni's multiple comparison test (Prism 5.0, GraphPad Software Inc., La Jolla, CA).

Chromatin immunoprecipitation (ChIP). Male wild-type and *Pparβ/δ*-null mice were treated with vehicle, GW0742, GSK3787, or GW0742 and GSK3787 by oral gavage 3 h prior to euthanasia as described above and colon and liver carefully dissected. Colon epithelium samples from five mice per group were individually snap frozen, pooled, and then pulverized using a mortar and pestle. Cross-linking was performed using a 1% formaldehyde saline solution with sample rotation for 10 min, after which the cross-linking was quenched by the addition of glycine to a final

MOL #65508

concentration of 125 mM and samples rotated for 10 min. Cells were washed twice with PBS before the addition of lysis buffer (50 mM Tris-HCl pH 8, 1% SDS, 10 mM EDTA, and protease inhibitor cocktail). The lysates from each treatment group were pooled, and the DNA was sheared to obtain sheared chromatin in the range of 500-1500 bp with the Diagenode Bioruptor™ (Diagenode, Sparta, NJ). The sheared chromatin was precleared by the addition of protein A agarose (Santa Cruz Biotechnology, Santa Cruz, CA) for 1 h that was previously blocked with bovine serum albumin (BSA)/salmon sperm DNA (Invitrogen, Carlsbad, CA). The precleared chromatin was immunoprecipitated by gentle agitation with specific antibodies for either anti-PPAR β/δ antibody (Girroir et al., 2008b), anti-acetylated histone H4 (Upstate Biotechnology, Lake Placid, NY) as a positive control, or rabbit IgG (Santa Cruz Biotechnology, Santa Cruz, CA) as a negative control. After 4 h, the immune complexes were captured by the addition of preblocked protein A agarose (Santa Cruz Biotechnology, Santa Cruz, CA) and overnight incubation. The beads were washed three times with a low salt wash buffer (20 mM Tris-HCl pH 8, 2 mM EDTA, 0.1% sodium deoxycholate, 1% Triton-X, 150 mM NaCl, and protease inhibitor cocktail) and once with a high salt wash buffer (20 mM Tris-HCl pH 8, 2 mM EDTA, 0.1% sodium deoxycholate, 1% Triton-X, 500 mM NaCl, and protease inhibitor cocktail). The beads were washed once with TE8 (10 mM Tris-HCl pH 8, 1 mM EDTA) and the immune complexes were released by the addition of elution buffer (100 mM NaHCO₃, 1% SDS). The formaldehyde cross-links were reversed by overnight incubation at 65°C. Immunoprecipitated DNA was purified by phenol/chloroform/isoamylalcohol (25:24:1) extraction and subject to real-time qPCR analysis for occupancy in the *Adrp* or *Angptl4* peroxisome proliferator response

MOL #65508

elements (PPRE). The *Adrp* PPRE (Chawla et al., 2003) and a primer set spanning this region have been previously described (Hollingshead et al., 2008). The primer set for *Angptl4* was designed based on previous identification of PPREs in intron 3 of the mouse *Angptl4* gene (Heinaniemi et al., 2007). The primers for *Angptl4* were 5'-CTAGCCAAGTAGAGGAAAGTTCAGAGC-3' (forward) and 5'-CCAATCCCTCGGGCAGCTAGC-3' (reverse). qPCR reactions were carried out as described above. The specific values were normalized to treatment inputs and verified to be greater than rabbit IgG controls. Promoter occupancy was determined based on fold accumulation to normalized vehicle values.

Reporter assays. The LexA-mPPAR β/δ , LexA-mPPAR α , LexA-mPPAR γ , 7L-TATA initiator module (TATAi) and PPRE-TATAi plasmids have been described previously (Fauti et al., 2005; Jerome and Muller, 1998; Naruhn et al., 2010). Transfections were performed with polyethylenimine (average MW 25,000; Sigma-Aldrich). NIH-3T3 cells were transfected on 6 well plates at 70- 80% confluence in Dulbecco's modified Eagle medium (DMEM) plus 2% fetal calf serum (FCS) with 5 μ g of plasmid DNA and 5 μ L of polyethylenimine (1:1000 dilution, adjusted to pH 7.0 and preincubated for 15 min in 200 μ L phosphate- buffered saline for complex formation). Four h after transfection, the medium was changed and cells were incubated in normal growth medium for 24 h with and without the presence of the PPAR α ligand GW7647 (0.3 μ M), the PPAR β/δ ligand GW501516 (0.3 μ M) the PPAR γ ligand GW1929 (0.3 μ M) and/or GSK3787 (1.0 μ M). Luciferase assays were performed as described (Gehrke et al., 2003). Values from three independent experiments were combined to calculate averages and standard deviations.

MOL #65508

Time resolved fluorescence resonance energy transfer (TR-FRET) assays

in vitro. The interaction of coregulator peptides with PPARs in vitro was determined by TR-FRET (Stafslien et al., 2007) using the Lanthascreen™ TR-FRET PPAR α , PPAR β/δ and PPAR γ coregulator assays according to the manufacturer's (Invitrogen, Carlsbad, CA) instructions with the following peptides: co-activator peptide C33, HVEMHPLLMLLMESQWGA; co-activator peptide thyroid hormone receptor-associated protein 220/vitamin D receptor interacting protein-1 (TRAP220/DRIP-1), KVSQNPILTSLLQITGNNG; co-repressor silencing mediator for retinoid and thyroid hormone receptors interaction domain 2 (SMRT-ID2), HASTNMGLEAIIRKALMGKYDQW; and nuclear receptor co-repressor interaction domain 2 (NCoR-ID2), DPASNLGLEDIIRKALMGSFDDK. Incubation times were 15-60 min for all assays shown in this study. The assay buffer contained 100 mM KCl, 20 mM Tris pH 7.9, 0.01% Triton X100 and 1 μ g/ μ L bovine serum albumin. All assays were validated for their robustness by determining the respective Z'-factors (Zhang et al., 1999). Measurements were performed on a VICTOR3V Multilabel Counter (WALLAC 1420; PerkinElmer, Waltham, MA) with instrument settings as described in the manufacturer's instructions for LanthaScreen™ assays.

Cell culture. The human hepatocarcinoma cell lines HepG2 and Huh7, lung adenocarcinoma cell lines A549 and H1838, squamous carcinoma cell line A431, and the breast cancer cell line MCF7 were obtained from American Type Culture Collection (Manassas, VA). Cells were cultured according to the recommended procedures: HepG2, Huh7, A431, and MCF7 cells were cultured in DMEM; A549 were cultured in Ham's F12K medium, and H1838 cells were cultured in RPMI-1640 medium

MOL #65508

supplemented with 10% fetal bovine serum (FBS) and 1% penicillin-streptomycin. For mRNA analysis, cells were plated in 12-well tissue culture plates, and cultured until 80% confluency at which time they were treated with either DMSO, GW0742, GSK3787 or GW0742 and GSK3787 for 24 h. The concentrations of GW0742 (0.05 – 1.0 μ M) were used because they have been previously shown to specifically activate PPAR β/δ (Shearer and Hoekstra, 2003). The concentrations of GSK3787 (0.1 – 10 μ M) were used because they have been previously shown to antagonize PPAR β/δ in other cell based models and are likely in the range of concentrations that could be achieved in vivo (Shearer et al., 2010). After this treatment, mRNA was isolated and used for qPCR as described above. Importantly, all of the cell lines have been shown to respond to ligand activation of PPAR β/δ and express PPAR β/δ mRNA (Girroi et al., 2008a; He et al., 2008; Hollingshead et al., 2007); and data not shown). However, relative expression of PPAR β/δ has been noted to be lower in these cancer cell lines as compared to normal cells/tissue (data not shown).

Isolation of mouse keratinocytes and fibroblasts. Keratinocytes and fibroblasts were isolated from newborn mouse skin and cultured as previously described (Dlugosz et al., 1995).

Cell proliferation assays. Cell proliferation was examined using real-time monitoring of cell proliferation of adherent cells using the xCELLigence System (Roche Applied Science, Indianapolis, IN). Briefly, the optimal number of cells required to obtain exponential growth in a single well of an E-Plate 16 was determined by monitoring cell proliferation in real time using increasing number of cells/well (Supplemental Fig. 1). The number of cells seeded per well to obtain exponential growth curves and the length

MOL #65508

of time examined for each cell line is shown in Supplemental Fig. 1. Cell proliferation was monitored every 15 min using the RTCES® system for up to 120 h. Cellsensor impedance is expressed as an arbitrary unit called the Cell Index. The Cell Index at each time point is defined as $(R_n - R_b)/15$, where R_n is the cell-electrode impedance of the well when it contains cells and R_b is the background impedance of the well with the media alone. Start and end times were selected during the log growth phase (Supplemental Fig. 1) and used to calculate doubling time with RTCA Software v 1.2 (ACEA Biosciences, Inc, San Diego, CA) from independent triplicate wells per treatment. For examination of the effect of GW0742 and/or GSK3787 on cell proliferation, the human squamous cell carcinoma cell line A431, human liver cancer cell lines HepG2, Huh7, human lung cancer cell lines A549, H1838 or the human breast cancer cell line MCF7 were seeded as described (Supplemental Fig. 1) and treated with GW0742 (0.1, 1.0 or 10 μ M) or GSK3787 (0.1, 1.0 or 10 μ M).

Quantitative Western Blotting. Protein samples were prepared from fibroblasts and keratinocytes using lysis buffer containing protease inhibitors. Seventy-five microgram of protein per sample was resolved using sodium dodecyl sulfate 10% polyacrylamide gels. Proteins were transferred onto a polyvinylidene fluoride membrane. The membrane was blocked with 5% non-fat milk or 0.5% gelatin in Tris buffered saline Tween (TBST) and incubated overnight with primary antibodies against PPAR β/δ (Girroir et al., 2008b) or lactate dehydrogenase (LDH). Membranes were washed and incubated with biotinylated secondary antibody (Jackson ImmunoResearch Laboratories, West Grove, PA) followed by incubation with ¹²⁵I-labeled streptavidin. Membranes were exposed to phosphorimager plates and the level of radioactivity

MOL #65508

quantified with a Packard phosphorimager. Hybridization signals for PPAR β/δ were normalized to the hybridization signals for the loading control LDH. Three independent samples were analyzed for each group.

3T3-L1 preadipocyte cell culture and differentiation. Mouse 3T3-L1 preadipocytes were cultured in DMEM with 10% FCS and 1% penicillin/streptomycin. Cells were cultured to confluence and then treated with differentiation medium. The differentiation medium was DMEM with 10% FBS, 10 μ g/mL insulin, 200 μ M 3-isobutyl-1-methylxanthine (IBMX) and 250 μ M dexamethasone. One day after treatment with the differentiation medium, cells were treated with 1.0 – 10 μ M rosiglitazone, 1.0 – 10 μ M GSK3787, or both rosiglitazone and GSK3787. For analysis of PPAR γ -dependent gene expression, RNA was isolated as described above from cells 24 h after treatment for analysis of the PPAR γ target gene *ap2* by qPCR as previously described by others (Rockwell et al., 2006). For analysis of adipocyte differentiation, cells were cultured for four days in maintenance medium containing DMEM with 10% FBS, 1% penicillin/streptomycin and insulin (10 μ g/mL) beginning 24 h after treatment with rosiglitazone, GSK3787 or both. Cells were fixed in 10% formalin and stained with Oil Red O (0.2% in 60% isopropanol) for 15 min. After washing with 60% isopropanol, Oil Red O stain was extracted with 4% NP-40 in isopropanol. The intensity of staining was determined by measuring absorbance at 570 nm.

Glucose tolerance test. Male wild-type and *Ppar β/δ* -null mice were administered GW0742, GSK3787 or rosiglitazone for 2 weeks as described above. After a six h fast, mice were injected with glucose (1.5 mg/g body weight) by intraperitoneal injection. After this injection, blood was collected from the mandibular vein every 30 min

MOL #65508

for 2 h and used for analysis of blood glucose using Accu-Chek® Active Glucometer (Roche Diagnostics, Indianapolis, IN).

Results

GSK3787 antagonizes ligand-induced PPAR β/δ -dependent gene expression in vivo. Preliminary characterization of GSK3787 indicated that this antagonist inhibits both basal and ligand-induced expression of pyruvate dehydrogenase kinase 4 (*PDK4*) and carnitine palmitoyl transferase 1a (*CPT1a*) in human skeletal muscle cells at concentrations up to 1 μ M (Shearer et al., 2010). Additionally, this study also demonstrated that oral administration of GSK3787 (10 mg/kg) led to a serum C_{\max} of 2.2 ± 0.4 μ M in C57BL/6 male mice (Shearer et al., 2010). To more definitively examine the effect of GSK3787 in vivo, qPCR analysis of PPAR β/δ target genes and ChIP assays were performed using tissue collected from wild-type and *Ppar β/δ* -null mice. Oral administration of GW0742 caused an increase in expression of *Angptl4* and *Adrp* mRNA (known PPAR β/δ target genes) in wild-type mouse colon epithelium, and this effect was not found in *Ppar β/δ* -null mouse colon epithelium (Fig. 2A). Oral administration of GSK3787 had no effect on expression of *Angptl4* and *Adrp* mRNA in mouse colon epithelium in either genotype (Fig. 2A). Co-administration of GSK3787 with GW0742 effectively prevented the ligand-induced expression of both *Angptl4* and *Adrp* mRNA in wild-type mouse colon epithelium and this effect was not found in *Ppar β/δ* -null mouse colon epithelium (Fig. 2A). GSK3787 did not modulate PPAR β/δ -dependent gene expression or antagonize ligand-induced PPAR β/δ -dependent gene expression in liver (data not shown). Since the antagonism of PPAR β/δ by GSK3787 was more evident in colon epithelium, consistent with high expression of PPAR β/δ in this tissue (Girroir et al., 2008b), ChIP assays were performed using colon epithelial

MOL #65508

DNA obtained from mice treated with either GW0742, GSK3787 or both compounds. Ligand activation of PPAR β/δ with GW0742 caused an increase in acetylated histone H4 (AcH4) associated with the PPRE region of both the *Angptl4* and *Adrp* genes in wild-type mouse colon epithelium and this effect was not found in similarly treated *Ppar β/δ* -null mice (Fig. 2B), consistent with past results (Hollingshead et al., 2008). Acetylation of histone H4 is important for chromatin remodeling and recruitment of the transcription initiation complex. While oral administration of GSK3787 had essentially no effect on promoter occupancy of AcH4 in the PPRE region of both the *Angptl4* and *Adrp* genes, co-administration of GSK3787 with GW0742 resulted in markedly less accumulation of AcH4 in the PPRE region of both the *Angptl4* and *Adrp* genes in wild-type mouse colon epithelium (Fig. 2B). Ligand activation of PPAR β/δ with GW0742 caused an increase in promoter occupancy of PPAR β/δ in the PPRE region of both the *Angptl4* and *Adrp* genes in wild-type mouse colon epithelium and this effect was not found in similarly treated *Ppar β/δ* -null mice (Fig. 2B). Oral administration of GSK3787 caused a modest increase in promoter occupancy of PPAR β/δ in the PPRE region of both the *Angptl4* and *Adrp* genes, but co-administration of GSK3787 with GW0742 resulted in markedly less accumulation of PPAR β/δ in the PPRE region of both the *Angptl4* and *Adrp* genes in wild-type mouse colon epithelium (Fig. 2B). These changes observed with co-administration were not found in similarly treated *Ppar β/δ* -null mouse colon epithelium. While promoter occupancy of AcH4 on the *Angptl4* gene was modestly lower in *Ppar β/δ* -null mouse colon epithelium following co-treatment with GW0742 and GSK3787, there was no change in promoter occupancy of AcH4 on the *Adrp* gene in *Ppar β/δ* -null mouse colon epithelium following co-treatment with GW0742 and

MOL #65508

GSK3787 (Fig. 2B). It remains possible that the former change could reflect an off-target effect of GSK3787 or a limitation due to the use of technical replicates for the ChIP assay, which precluded assessing measures of variability. Collectively, these results demonstrate that GSK3787 can effectively antagonize ligand-induced effects on PPAR β/δ target genes in vivo, and that these effects are due to receptor-dependent mechanisms since they are not found in *Ppar β/δ* -null mice.

GSK3787 antagonizes ligand-induced PPAR β/δ -dependent gene expression in vitro. While preliminary characterization of GSK3787 indicates that this compound can antagonize both basal and ligand-induced expression of *PDK4* and *CPT1a* in human skeletal muscle cells at concentrations up to 1 μ M (Shearer et al., 2010), the specificity of this effect on gene expression was not examined. For this reason, the effect of GSK3787 in cells expressing a relatively low level of PPAR β/δ (fibroblasts) and a relatively high level of PPAR β/δ (keratinocytes) was examined using cells isolated from wild-type and *Ppar β/δ* -null mice. Expression of PPAR β/δ protein is ~7-fold lower in fibroblasts as compared to keratinocytes (Fig. 3A). Keratinocytes are known to express PPAR β/δ at a high level as compared to most other mouse tissues/cells (Girroir et al., 2008b). Despite the relatively low level of expression of PPAR β/δ observed in fibroblasts, treatment with 10 or 50 nM GW0742 caused up to ~10-fold increase of *Angptl4* mRNA compared to control; this effect was not found in fibroblasts from *Ppar β/δ* -null mice (Fig. 3B). The increase in *Angptl4* mRNA observed in response to 10 nM GW0742 was not found in wild-type fibroblasts that were cultured with both 10 nM GW0742 and 0.1 or 1.0 μ M GSK3787 (Fig. 3B). The increase in *Angptl4* mRNA observed in response to 50 nM GW0742 was markedly lower in wild-type fibroblasts

MOL #65508

that were cultured with 50 nM GW0742 and 0.1 μ M GSK3787 and essentially absent in wild-type fibroblasts that were cultured with 50 nM GW0742 and 1.0 μ M GSK3787 (Fig. 3B). None of these effects were found in similarly treated fibroblasts from *Ppar β / δ* -null mice (Fig. 3B). Consistent with the difference in expression of PPAR β / δ protein (Fig. 3A), the change in expression of *Angptl4* mRNA in response to GW0742 was greater in keratinocytes as compared to fibroblasts as 50 nM GW0742 caused greater than a 30-fold increase in *Angptl4* mRNA compared to control (Fig. 3C). The increase in *Angptl4* mRNA observed in response to 50 nM GW0742 was markedly lower in wild-type keratinocytes that were cultured with 50 nM GW0742 and 0.1 μ M GSK3787 and not found in wild-type keratinocytes that were cultured with 50 nM GW0742 and 1.0 μ M GSK3787 (Fig. 3C). None of these changes were found in similarly treated keratinocytes from *Ppar β / δ* -null mice (Fig. 3C). Combined, these results establish that GSK3787 can effectively antagonize ligand-induced gene expression mediated by PPAR β / δ in cultured fibroblasts and keratinocytes using concentrations ranging from 0.1 – 1.0 μ M in the presence of an agonist with affinity for PPAR β / δ in the nM range.

GSK3787 antagonizes ligand-induced PPAR β / δ -dependent gene expression in human cancer cell lines. There is considerable interest in the effect of PPAR β / δ in human cancer (reviewed in Burdick et al., 2006; Peters and Gonzalez, 2009; Peters et al., 2008). Thus, the relative ability of GSK3787 to antagonize PPAR β / δ was examined in a panel of human cancer cell lines including those for skin (A431), liver (HepG2, Huh7), breast (MCF7) and lung cancer (H1838, A549). Expression of *ANGPTL4* and *ADRP* mRNAs in A431 cells were increased by ~20-fold and ~6-fold, respectively, by 50 nM GW0742 (Fig. 4). Co-treatment with 50 nM GW0742 and 1.0 μ M GSK3787 largely

MOL #65508

diminished these GW0742-induced responses in A431 cells (Fig. 4). The magnitude of ligand-induced changes in PPAR β/δ target genes was greater in A431 cells as compared to the other human cancer lines. Treatment with 50 nM GW0742 caused an increase in expression of *ANGPTL4* mRNA in MCF7, Huh7, HepG2, H1838 and A549 cells ranging from ~2-fold to 6-fold (Fig. 4). The magnitude of change in GW0742-induced *ANGPTL4* mRNA expression in these cells was markedly lower as compared to primary mouse keratinocytes, where >30-fold increases were noted (Fig. 3C). Co-treatment of 50 nM GW0742 and 1.0 μ M GSK3787 antagonized the GW0742-induced increase of *ANGPTL4* mRNA in MCF7, Huh7 and HepG2 cells but not in H1838 or A549 cells (Fig. 4). *ADRP* mRNA increased following treatment with 50 nM GW0742 in Huh7, HepG2 and H1838 cells but not in MCF7 or A549 cells (Fig. 4). Co-treatment of 50 nM GW0742 and 1.0 μ M GSK3787 antagonized the GW0742-induced increase of *ADRP* mRNA in Huh7 and HepG2 cells but not in H1838 cells (Fig. 4). These data show that GSK3787 can antagonize ligand-induced changes in gene expression in most, but not all, human cancer cell lines examined in this study. This is in contrast to effective antagonism of ligand-induced changes in gene expression observed in mouse primary fibroblasts and keratinocytes using the same concentrations of GW0742 and GSK3787 (Fig. 3B, 3C). No decrease in basal expression of either *ANGPTL4* or *ADRP* mRNA was observed following treatment with GSK3787 suggesting that GSK3787 does not antagonize basal expression of either of these two PPAR β/δ target gene in A431, MCF7, Huh7, HepG2, H1838 or A549 human cancer cell lines.

Effect of ligand activation of PPAR β/δ by GW0742 and antagonism of PPAR β/δ by GSK3787 on cell proliferation. There is considerable controversy

MOL #65508

regarding the effects of PPAR β/δ on the proliferation of cultured human cancer cells as there is evidence that PPAR β/δ either increases, decreases or has no effect on cell growth (reviewed in Burdick et al., 2006; Peters and Gonzalez, 2009; Peters et al., 2008). Thus, the effect of GW0742 and/or GSK3787 on cell proliferation was examined in the human cancer cell lines A431, HepG2, Huh7, MCF7, H1838, and A549. Neither GW0742 nor GSK3787 had any effect on cell proliferation in MCF7, Huh7, HepG2, A431, A549 or H1838 human cancer cell lines at concentrations ranging from 0.1 – 10 μ M (Table 1).

GSK3787 selectively antagonizes ligand-induced PPAR β/δ transcription but also modulates PPAR γ activities. Reporter assays were performed to determine if GSK3787 could activate the two other members of the PPAR family, PPAR α and PPAR γ . GSK3787 did not modulate PPAR α -dependent trans-activation and had no effect on ligand-induced trans-activation of PPAR α by GW7647 (Fig. 5). In contrast, GW501516-induced PPAR β/δ -dependent trans-activation was effectively antagonized by GSK3787 (Fig. 5). Interestingly, GSK3787 was able to modestly increase PPAR γ -dependent reporter activity as compared to the PPAR γ agonist GW1929 (Fig. 5). Additionally, GSK3787 also antagonized GW1929-induced PPAR γ trans-activation (Fig. 5). These data revealed that GSK3787 had no influence on PPAR α activity, is effective as a PPAR β/δ antagonist, and weak PPAR γ agonistic and antagonistic activities.

To more closely examine the ability of GSK3787 to antagonize PPAR activity, the interaction between PPAR β/δ , PPAR γ and co-activator or co-repressor peptides was determined using TR-FRET. In this assay, the interaction between the PPAR β/δ or PPAR γ ligand binding domain (LBD; indirectly labeled with terbium) with either, the co-

MOL #65508

activator peptides C33 or TRAP220/DRIP-1 (labeled with fluorescein), or the co-repressor peptides SMRT ID2 or NCoR ID2 (labeled with fluorescein) was determined. The in vitro TR-FRET assay measures the intensity of terbium-induced fluorescence emission of the fluorescein moiety of the labeled peptides, expressed as the ratio of fluorescein- and terbium-derived fluorescence. In the absence of ligand (GW501516), GSK3787 decreased co-repressor peptide SMRT ID2 dissociation at higher concentrations (0.75 and 1.0 μM) and dose-dependently decreased recruitment of co-activator peptide C33 to the PPAR β/δ LBD (Fig. 6A, 6C). In the absence of ligand, GSK0660 did not influence co-repressor peptide SMRT ID2 dissociation but did decrease recruitment of co-activator peptide C33 to the PPAR β/δ LBD (Fig. 6A, 6C). Previous studies established that maximal SMRT ID2 dissociation from, and maximal C33 recruitment with, the LBD of PPAR β/δ occurs by 30 min post-ligand treatment (data not shown). A dose dependent prevention of co-repressor peptide SMRT ID2 dissociation (Fig. 6B) and inhibition of co-activator peptide C33 recruitment (Fig. 6D) was observed following co-treatment of 0.15 μM GW501516 with GSK3787. Similar changes in PPAR β/δ LBD/co-activator/co-repressor interactions were not observed with co-treatment of GW501516 with GSK0660, another PPAR β/δ antagonist (Fig. 6B, 6D). Since the reporter assays (Fig. 5) indicated that GSK3787 also modulates PPAR γ activity, TR-FRET assays were performed to compare co-regulator peptide recruitment/dissociation between PPAR γ and PPAR β/δ . In the absence of ligand (GW501516), GSK3787 caused dissociation of co-repressor peptides SMRT ID2 and NCoR ID2 from the PPAR β/δ LBD but had no effect on recruitment of the PPAR γ co-activator TRAP220/DRIP-1 to the PPAR β/δ LBD (Fig. 7A). GSK0660 had no effect on

MOL #65508

either dissociation of co-repressor peptides SMRT ID2 or NCoR ID2 from the PPAR β/δ LBD, or recruitment of the PPAR γ co-activator TRAP220/DRIP-1 to the PPAR β/δ LBD (Fig. 7A). In the absence of ligand (GW1929), GSK3787 and GSK0660 caused some dissociation of co-repressor peptides SMRT ID2 but not NCoR ID2 from the PPAR γ LBD (Fig. 7B). In the absence of ligand, GSK3787 enhanced recruitment of the PPAR γ co-activator TRAP220/DRIP-1 to the PPAR γ LBD, while GSK0660 had no effect on recruitment of TRAP220/DRIP-1 to the PPAR γ LBD (Fig. 7B). GW501516-induced recruitment of TRAP220/DRIP-1 to the PPAR β/δ LBD and dissociation of SMRT ID2 from the PPAR β/δ LBD were both inhibited by GSK3787, and GSK0660 did not influence either of these effects (Fig. 7C). Interestingly, GW1929-induced recruitment of TRAP220/DRIP-1 to the PPAR γ LBD and dissociation of SMRT ID2 from the PPAR γ LBD were both inhibited by GSK3787 and GSK0660 did not change either of these effects (Fig. 7D). Combined, these data suggest that while GSK3787 can antagonize PPAR β/δ , this compound can also cause molecular interactions between co-activators and co-repressor peptides with the LBD of PPAR γ , similar to effects found with PPAR γ agonists and antagonists, consistent with the reporter assays (Fig. 5).

To begin to determine the relative efficacy of GSK3787 to modulate PPAR γ activity, the effect of GSK3787 to regulate PPAR γ -dependent gene expression was examined in an adipocyte cell-based model. 3T3-L1 preadipocytes were cultured with adipocyte differentiation medium to enhance PPAR γ activity and then treated with either, a PPAR γ agonist (rosiglitazone), GSK3787 or rosiglitazone and GSK3787. Expression of the PPAR γ target gene *ap2* mRNA was markedly increased by treatment with 1 or 10 μ M rosiglitazone (Fig. 8). GSK3787 (1 or 10 μ M) had no effect on

MOL #65508

expression of *ap2* mRNA in 3T3-L1 cells and did not antagonize rosiglitazone-induced expression of *ap2* mRNA (Fig. 8). Similarly, rosiglitazone caused an increase in lipid accumulation associated with adipocyte differentiation as shown by Oil Red O staining, whereas GSK3787 did not significantly influence Oil Red O staining or modulate the increase in adipocyte differentiation caused by rosiglitazone (Fig. 8C, Supplemental Fig. 2). These data suggest that the efficacy of GSK3787 to activate PPAR γ is markedly lower as compared to rosiglitazone. These data also suggest that the efficacy of GSK3787 to antagonize PPAR γ -dependent gene expression is markedly less as compared to its ability to antagonize PPAR β/δ -dependent gene expression.

Effect of GSK3787 on glucose tolerance. Ligand activation of PPAR β/δ or PPAR γ can both improve insulin sensitivity and glucose tolerance (reviewed in Quinn et al., 2008; Reilly and Lee, 2008). Since GSK3787 may modulate both PPAR β/δ and/or PPAR γ activities, the effect of GSK3787 on glucose tolerance was examined. Higher blood glucose, consistent with glucose intolerance, was observed in *Ppar β/δ* -null mice as compared to wild-type mice, similar with past results (Lee et al., 2006). Treatment with GW0742 for 2 weeks markedly improved glucose tolerance in wild-type mice and this effect was not found in GW0742-treated *Ppar β/δ* -null mice (Fig. 9). In contrast, treatment with rosiglitazone for 2 weeks improved glucose tolerance in both wild-type and *Ppar β/δ* -null mice (Fig. 9). Administration of GSK3787 had no effect on glucose tolerance in either genotype (Fig. 9).

Discussion

These studies are the first to demonstrate that GSK3787 can effectively antagonize ligand-induced effects on PPAR β/δ target genes in vivo through receptor-dependent mechanisms since they are not found in *Ppar β/δ* -null mice. This conclusion is supported by qPCR analysis demonstrating PPAR β/δ -dependent antagonism of ligand-induced changes in gene expression in colon epithelium, as well as ChIP assays demonstrating PPAR β/δ -dependent antagonism of ligand-induced promoter occupancy of PPAR β/δ on target genes in colon epithelium. Further confirmation of receptor-specificity for at least some GSK3787 activity was provided by results showing that GSK3787 can antagonize GW0742-induced changes in gene expression in wild-type mouse fibroblasts and keratinocytes, but not in *Ppar β/δ* -null cells. It is noteworthy that GSK3787 caused no overt signs of toxicity as assessed by relative cell proliferation. The specificity of GSK3787 for PPAR β/δ could be due in part to the fact that it is an irreversible antagonist that forms a covalent bond within the ligand binding domain of PPAR β/δ (Shearer et al., 2010). GSK3787 also antagonized ligand-induced changes in gene expression in most, but not all human cancer cell lines examined in this study. This is in contrast to PPAR β/δ -dependent antagonism by GSK3787 of ligand-induced changes in gene expression observed in mouse fibroblasts and keratinocytes using the same concentrations of GW0742 and GSK3787. Determining the mechanisms for the resistance of the human lung cancer cell lines H1838 and A549 to PPAR β/δ antagonism by GSK3787 requires further study.

MOL #65508

It is worth noting that potency and efficacy of ligand activation of PPAR β/δ on target gene expression in fibroblasts and keratinocytes were markedly greater as compared to MCF7, Huh7, HepG2, H1838 and A549 cells. This suggests that the ability of a ligand to activate PPAR β/δ is relatively less in these human cancer cell lines as compared to mouse fibroblasts and keratinocytes. While the mechanism for this difference is not known, the ligand may be more rapidly degraded in the latter cell lines as compared to fibroblasts and keratinocytes. Further, since GSK3787 antagonized ligand-induced gene expression in mouse fibroblasts and keratinocytes that express relatively low and relatively high levels of PPAR β/δ protein, respectively, this demonstrates that GSK3787 is effective for in vitro models at concentrations ranging from 0.1 – 1.0 μ M in cells with varying levels of receptor expression. This is important to point out because these concentrations are comparable to concentrations achievable in vivo since the C_{\max} in serum observed in mice administered GSK3787 (10 mg/kg) is 2.2 ± 0.4 μ M with a half life of 2.5 ± 1.1 h (Shearer et al., 2010). In model systems that lack the presence of high affinity ligands, but are dependent on endogenous lower affinity ligands (e.g. fatty acids, fatty acid derivatives), concentrations of GSK3787 between 0.1 – 1.0 μ M should be capable of antagonizing constitutive PPAR β/δ function. Thus, it is surprising that GSK3787 has no effect on basal expression of PPAR β/δ target genes examined in these studies in fibroblasts, keratinocytes or human cancer cell lines. This is in contrast to reduced basal expression of *CPT1a* and *PDK4* in human skeletal muscle cells observed following treatment with GSK3787 (Shearer et al., 2010). This could be due to differences in regulatory elements in the promoters between *CPT1a* or

MOL #65508

PDK4 and *ANGPTL4* or *ADRP*. Future in vivo and in vitro studies should consider this possibility.

Despite demonstrating that GSK3787 specifically antagonizes ligand-induced activity of PPAR β/δ based on analysis of cells and mice lacking expression of PPAR β/δ , evidence was also obtained demonstrating that GSK3787 has weak PPAR γ agonist and antagonist activities. However, comparison of PPAR γ function in 3T3-L1 cells demonstrated negligible PPAR γ agonistic or antagonistic activities by GSK3787 as shown by both the lack of change in expression of a known PPAR γ target gene and analysis of adipocyte differentiation. Since the concentrations required to specifically antagonize PPAR β/δ are less than or equal to 1 μ M, and this concentration of GSK3787 did not cause significant agonism or antagonism of PPAR γ activity in 3T3-L1 adipocytes, this suggests that GSK3787 can be used to study the effects of PPAR β/δ antagonism in vitro without considering confounding changes due to PPAR γ -dependent activity; as suggested by the FRET analysis and reporter assays that may exhibit increased sensitivity. In vivo examination of glucose tolerance also demonstrated negligible PPAR γ activity of GSK3787 as compared to a known PPAR γ agonist using a dose of GSK3787 that effectively antagonized ligand-induced PPAR β/δ transcriptional activity in colonic epithelium. However, it is important to emphasize that experiments should control for this potential PPAR γ agonism/antagonism by GSK3787, as it remains possible that other PPAR γ -dependent activities could influence interpretation. Further, whether GSK3787 can be used as an antagonist to study ligand-induced improvement of insulin sensitivity mediated by PPAR β/δ requires further examination.

MOL #65508

Results from these studies also illustrate differences in functional roles of PPAR β/δ in cell proliferation. There is considerable controversy regarding the role of PPAR β/δ in cell proliferation as some studies suggest that activating this receptor increases cell proliferation while others indicate that activating PPAR β/δ has either no effect, or inhibits cell proliferation in association with the induction of terminal differentiation (reviewed in Peters and Gonzalez, 2009; Peters et al., 2008). This is largely due to the lack of stringency in approaches used to examine cell proliferation, in particular the limited published time course and concentration-dependent studies. Ligand activation of PPAR β/δ with GW0742 had no effect on cell proliferation in A431, MCF7, Huh7, HepG2, H1838 or A549 human cancer cell lines, results that are consistent with some, but not all studies, showing that GW0742 or GW501516 have little influence on cell proliferation at concentrations less than 10 μ M (reviewed in Peters and Gonzalez, 2009; Peters et al., 2008). The present studies examined cell proliferation by determining doubling time using real-time analysis, and many published studies typically limit analysis of cell proliferation to a single timepoint (reviewed in Peters and Gonzalez, 2009; Peters et al., 2008). Thus, it remains possible that the approach used to detect cell growth could impact these findings. Importantly, real-time analysis of cell proliferation provides an outstanding approach yielding accurate assessment of doubling time during the linear growth phase over a broad concentration range of compound. Since ligand activation of PPAR β/δ had no influence on cell proliferation, it is not surprising that GSK3787 had no effect on cell proliferation in A431, MCF7, Huh7, HepG2, H1838 or A549 human cancer cell lines, despite the fact that GSK3787 antagonized ligand-induced changes in PPAR β/δ -dependent gene

MOL #65508

expression in these cells. This is consistent with a recent study where GSK3787 had no effect on cell proliferation in SW480, HCT116, DLD1, RKO, A549 or HEK293 cancer cell lines with concentrations of GSK3787 up to 10 μ M (Shearer et al., 2010). This could be due to the fact that expression of PPAR β/δ is low in tumors and cancer cell lines as compared to “normal” cells. For example, expression of PPAR β/δ in the C20 mammary gland cancer cell line is less than 25% of that found in keratinocytes (Foreman et al., 2010). Further, while it has been suggested that PPAR β/δ expression is up-regulated by the APC/ β -CATENIN signaling pathway that is often enhanced in cancer, recent findings indicate that this idea is incorrect (Foreman et al., 2009) and many studies show that PPAR β/δ expression is either lower or unchanged in tumors as compared to control tissue (Berglund et al., 2008; Uhlen et al., 2005; reviewed in Peters and Gonzalez, 2009; Peters et al., 2008). Thus, while activation of PPAR β/δ with a high affinity ligand modulates changes in gene expression in cancer cell lines, the effect of either an agonist or an antagonist on cell proliferation can be negligible in human cancer cell lines.

Results from these studies are in contrast to a recent report suggesting that antagonism of PPAR β/δ with 10 μ M SR13904 inhibited cell proliferation of A549 cells (Zaveri et al., 2009). However, data from the present study and recent work by others (Shearer et al., 2010) show that antagonism of PPAR β/δ in the same human lung cancer cell line has no effect on cell proliferation at concentrations that specifically antagonize PPAR β/δ . It is important to note that the study by Zaveri et al had limitations that preclude definitive conclusions regarding the specificity of the response observed with SR13904 since they did not demonstrate an increase in A549 cell growth by ligand

MOL #65508

activation of PPAR β/δ that was prevented by co-treatment with SR13904. This is a concern since no effect on cell proliferation is found in response to ligand activation of PPAR β/δ in A549 cells as shown by the present study and another recent report (He et al., 2008). Moreover, Zaveri et al did not demonstrate specific antagonism of ligand-induced PPAR β/δ target gene(s) or altered cell proliferation using knockout or knockdown approaches. This raises the possibility that the observed inhibition of cell proliferation in A549 cells by high concentration SR13904 is due to off target effects rather than antagonism of PPAR β/δ , in particular since SR13904 was also shown to antagonize PPAR γ (Zaveri et al., 2009).

While it has been suggested that antagonism of PPAR β/δ may be a useful approach for chemoprevention (Zuo et al., 2009), this idea is not supported by results from the present study showing no influence on cell proliferation of human cancer cell lines and the fact that the effect of ligand activation of PPAR β/δ on tumorigenesis is entirely unclear (reviewed in Peters and Gonzalez, 2009; Peters et al., 2008). Further, since ligand activation of PPAR β/δ improves insulin sensitivity, increases skeletal muscle fatty acid catabolism, and has potent anti-inflammatory activities, therapeutic antagonism of PPAR β/δ could likely lead to negative effects on these essential functions. Nevertheless, results from these studies demonstrate that GSK3787 can be used to antagonize PPAR β/δ in vivo and in vitro, providing a new strategy to delineate the functional role of a receptor with great potential as a therapeutic target for the treatment and prevention of diseases including dyslipidemias, obesity and cancer. Given the potential for GSK3787 to interact with PPAR γ , receptor specificity must be controlled for in future studies.

MOL #65508

Acknowledgements. The authors gratefully acknowledge Andrew Billin and Timothy Willson for providing GW0742, GSK0660 and GSK3787.

MOL #65508

References

- Barak Y, Liao D, He W, Ong ES, Nelson MC, Olefsky JM, Boland R and Evans RM (2002) Effects of peroxisome proliferator-activated receptor δ on placentation, adiposity, and colorectal cancer. *Proc Natl Acad Sci U S A* **99**:303-308.
- Billin AN (2008) PPAR- β/δ agonists for Type 2 diabetes and dyslipidemia: an adopted orphan still looking for a home. *Expert opinion on investigational drugs* **17**(10):1465-1471.
- Burdick AD, Kim DJ, Peraza MA, Gonzalez FJ and Peters JM (2006) The role of peroxisome proliferator-activated receptor- β/δ in epithelial cell growth and differentiation. *Cell Signal* **18**(1):9-20.
- Chawla A, Lee CH, Barak Y, He W, Rosenfeld J, Liao D, Han J, Kang H and Evans RM (2003) PPAR δ is a very low-density lipoprotein sensor in macrophages. *Proc Natl Acad Sci U S A* **100**(3):1268-1273.
- Dlugosz AA, Glick AB, Tennenbaum T, Weinberg WC and Yuspa SH (1995) Isolation and utilization of epidermal keratinocytes for oncogene research. *Methods Enzymol* **254**:3-20.
- Fauti T, Müller-Brüsselbach S, Kreutzer M, Rieck M, Meissner W, Rapp U, Schweer H, Kömhoff M and Müller R (2005) Induction of PPAR β and prostacyclin (PGI₂) synthesis by Raf signaling: failure of PGI₂ to activate PPAR β . *Febs J* **273**(1):170-179.
- Foreman JE, Sharma AK, Amin S, Gonzalez FJ and Peters JM (2010) Ligand activation of peroxisome proliferator-activated receptor- β/δ (PPAR β/δ) inhibits cell growth in a mouse mammary gland cancer cell line. *Cancer Lett* **288**:219-225.

MOL #65508

- Foreman JE, Sorg JM, McGinnis KS, Rigas B, Williams JL, Clapper ML, Gonzalez FJ and Peters JM (2009) Regulation of peroxisome proliferator-activated receptor- β/δ by the APC/ β -CATENIN pathway and nonsteroidal antiinflammatory drugs. *Mol Carcinog* **48**(10):942-952.
- Gehrke S, Jerome V and Muller R (2003) Chimeric transcriptional control units for improved liver-specific transgene expression. *Gene* **322**:137-143.
- Girroir EE, Hollingshead HE, Billin AN, Willson TM, Robertson GP, Sharma AK, Amin S, Gonzalez FJ and Peters JM (2008a) Peroxisome proliferator-activated receptor- β/δ (PPAR β/δ) ligands inhibit growth of UACC903 and MCF7 human cancer cell lines. *Toxicology* **243**(1-2):236-243.
- Girroir EE, Hollingshead HE, He P, Zhu B, Perdew GH and Peters JM (2008b) Quantitative expression patterns of peroxisome proliferator-activated receptor- β/δ (PPAR β/δ) protein in mice. *Biochem Biophys Res Commun* **371**(3):456-461.
- Gross B and Staels B (2007) PPAR agonists: multimodal drugs for the treatment of type-2 diabetes. *Best practice & research* **21**(4):687-710.
- He P, Borland MG, Zhu B, Sharma AK, Amin S, El-Bayoumy K, Gonzalez FJ and Peters JM (2008) Effect of ligand activation of peroxisome proliferator-activated receptor- β/δ (PPAR β/δ) in human lung cancer cell lines. *Toxicology* **254**:112-117.
- Heinaniemi M, Uski JO, Degenhardt T and Carlberg C (2007) Meta-analysis of primary target genes of peroxisome proliferator-activated receptors. *Genome Biol* **8**(7):R147.
- Hollingshead HE, Borland MG, Billin AN, Willson TM, Gonzalez FJ and Peters JM (2008) Ligand activation of peroxisome proliferator-activated receptor- β/δ

MOL #65508

(PPAR β/δ) and inhibition of cyclooxygenase 2 (COX2) attenuate colon carcinogenesis through independent signaling mechanisms. *Carcinogenesis* **29**(1):169-176.

Hollingshead HE, Killins RL, Borland MG, Girroir EE, Billin AN, Willson TM, Sharma AK, Amin S, Gonzalez FJ and Peters JM (2007) Peroxisome proliferator-activated receptor- β/δ (PPAR β/δ) ligands do not potentiate growth of human cancer cell lines. *Carcinogenesis* **28**(12):2641-2649.

Jerome V and Muller R (1998) Tissue-specific, cell cycle-regulated chimeric transcription factors for the targeting of gene expression to tumor cells. *Human gene therapy* **9**(18):2653-2659.

Lee CH, Olson P, Hevener A, Mehl I, Chong LW, Olefsky JM, Gonzalez FJ, Ham J, Kang H, Peters JM and Evans RM (2006) PPAR δ regulates glucose metabolism and insulin sensitivity. *Proc Natl Acad Sci U S A* **103**(9):3444-3449.

Nadra K, Anghel SI, Joye E, Tan NS, Basu-Modak S, Trono D, Wahli W and Desvergne B (2006) Differentiation of trophoblast giant cells and their metabolic functions are dependent on peroxisome proliferator-activated receptor β/δ . *Mol Cell Biol* **26**(8):3266-3281.

Naruhn S, Meissner W, Adhikary T, Kaddatz K, Klein T, Watzer B, Muller-Brusselbach S and Muller R (2010) 15-hydroxyeicosatetraenoic acid is a preferential peroxisome proliferator-activated receptor β/δ agonist. *Mol Pharmacol* **77**(2):171-184.

MOL #65508

Peters JM and Gonzalez FJ (2009) Sorting out the functional role(s) of peroxisome proliferator-activated receptor- β/δ (PPAR β/δ) in cell proliferation and cancer.

Biochim Biophys Acta **1796**(2):230-241.

Peters JM, Hollingshead HE and Gonzalez FJ (2008) Role of peroxisome-proliferator-activated receptor β/δ (PPAR β/δ) in gastrointestinal tract function and disease.

Clin Sci (Lond) **115**(4):107-127.

Peters JM, Lee SST, Li W, Ward JM, Gavrilova O, Everett C, Reitman ML, Hudson LD and Gonzalez FJ (2000) Growth, adipose, brain and skin alterations resulting from targeted disruption of the mouse peroxisome proliferator-activated receptor β/δ . *Molecular and Cellular Biology* **20**:5119-5128.

Quinn CE, Hamilton PK, Lockhart CJ and McVeigh GE (2008) Thiazolidinediones: effects on insulin resistance and the cardiovascular system. *British journal of pharmacology* **153**(4):636-645.

Reilly SM and Lee CH (2008) PPAR δ as a therapeutic target in metabolic disease. *FEBS Lett* **582**(1):26-31.

Rockwell CE, Snider NT, Thompson JT, Vanden Heuvel JP and Kaminski NE (2006) Interleukin-2 suppression by 2-arachidonyl glycerol is mediated through peroxisome proliferator-activated receptor gamma independently of cannabinoid receptors 1 and 2. *Mol Pharmacol* **70**(1):101-111.

Shearer BG and Hoekstra WJ (2003) Recent advances in peroxisome proliferator-activated receptor science. *Curr Med Chem* **10**(4):267-280.

Shearer BG, Steger DJ, Way JM, Stanley TB, Lobe DC, Grillot DA, Iannone MA, Lazar MA, Willson TM and Billin AN (2008) Identification and characterization of a

MOL #65508

selective peroxisome proliferator-activated receptor β/δ (NR1C2) antagonist. *Mol Endocrinol* **22**(2):523-529.

Shearer BG, Wiethe RW, Ashe A, Billin AN, Way JM, Stanley TB, Wagner CD, Xu RX, Leesnitzer LM, Merrihew RV, Shearer TW, Jeune MR, Ulrich JC and Willson TM (2010) Identification and Characterization of 4-Chloro-N-(2-([5-trifluoromethyl]-2-pyridyl)sulfonyl)ethyl)benzamide (GSK3787), a Selective and Irreversible Peroxisome Proliferator-Activated Receptor δ (PPAR δ) Antagonist. *J Med Chem* **53**(4):1857-1861.

Staels B, Dallongeville J, Auwerx J, Schoonjans K, Leitersdorf E and Fruchart JC (1998) Mechanism of action of fibrates on lipid and lipoprotein metabolism. *Circulation* **98**(19):2088-2093.

Stafslien DK, Vedvik KL, De Rosier T and Ozers MS (2007) Analysis of ligand-dependent recruitment of coactivator peptides to RXR β in a time-resolved fluorescence resonance energy transfer assay. *Mol Cell Endocrinol* **264**(1-2):82-89.

Sznajdman ML, Haffner CD, Maloney PR, Fivush A, Chao E, Goreham D, Sierra ML, LeGrumelec C, Xu HE, Montana VG, Lambert MH, Willson TM, Oliver WR and Sternbach DD (2003) Novel selective small molecule agonists for peroxisome proliferator-activated receptor δ (PPAR δ)-synthesis and biological activity. *Bioorg Med Chem Lett* **13**(9):1517-1521.

Zaveri NT, Sato BG, Jiang F, Calaoagan J, Laderoute KR and Murphy BJ (2009) A novel peroxisome proliferator-activated receptor δ antagonist, SR13904, has

MOL #65508

anti-proliferative activity in human cancer cells. *Cancer Biol Ther* **8**(13):1252-1261.

Zhang JH, Chung TD and Oldenburg KR (1999) A Simple Statistical Parameter for Use in Evaluation and Validation of High Throughput Screening Assays. *J Biomol Screen* **4**(2):67-73.

Zuo X, Peng Z, Moussalli MJ, Morris JS, Broaddus RR, Fischer SM and Shureiqi I (2009) Targeted genetic disruption of peroxisome proliferator-activated receptor- δ and colonic tumorigenesis. *J Natl Cancer Inst* **101**(10):762-767.

MOL #65508

Footnotes. This work is supported by the National Institutes of Health [CA124533, CA126826, CA141029], the Deutsche Forschungsgemeinschaft [SFB-TR17/A3], and the Intramural Research Program of the National Institutes of Health, National Cancer Institute. Reprint requests to: Dr. Jeffrey M. Peters, Department of Veterinary and Biomedical Sciences and The Center for Molecular Toxicology and Carcinogenesis, The Pennsylvania State University, University Park, PA 16802. Email: jmp21@psu.edu

MOL #65508

Figure Legends:

Fig. 1. Chemical structure of 4-chloro-N-(2-([5-trifluoromethyl]-2-pyridyl)sulfonyl)ethyl)benzamide (GSK3787).

Fig. 2. GSK3787 antagonizes ligand-induced changes in PPAR β/δ -dependent gene expression in vivo. Wild-type (~) or *Ppar* β/δ -null (–/–) mice were treated with the PPAR β/δ ligand GW0742 (10 mg/kg), the PPAR β/δ antagonist GSK3787 (10 mg/kg), or both GW0742 and GSK3787 (both at 10 mg/kg) as described in *Materials and Methods*. (A) Quantitative real-time PCR was performed using total RNA isolated from colon epithelium to quantify mRNA expression of the PPAR β/δ target genes *Angptl4* or *Adrp*. Values are the average normalized fold change as compared to vehicle control and represent the mean \pm S.E.M. N = 4 biological replicates. Values with different letters are significantly different, $P \leq 0.05$, as determined by ANOVA and Bonferroni's multiple comparison test. (B) Chromatin immunoprecipitations were carried out as described in *Material and Methods* to examine the recruitment of PPAR β/δ and histone acetylation at the regulatory regions of *Angptl4* (left panels) and *Adrp* (right panel) in chromatin isolated from colon epithelium from ~) and (–/–). Values are the input normalized average of technical replicates as fold change compared to vehicle control. N = 1 technical replicate of 5 pooled biological replicates.

Fig. 3. GSK3787 antagonizes ligand-induced changes in PPAR β/δ -dependent gene expression in mouse primary fibroblasts and keratinocytes. (A) Expression of PPAR β/δ

MOL #65508

protein in keratinocytes and fibroblasts from wild-type (++) or *Pparβ/δ*-null (−/−) mice. Normalized expression values are fold expression relative to keratinocytes and represent the mean ± S.E.M.. N = 3 biological replicates. Expression of PPARβ/δ is ~7-fold lower in fibroblasts as compared to keratinocytes. + = positive control (lysate from COS1 cells transfected with PPARβ/δ expression vector. N.D. = not detected. (B) Fibroblasts or (C) keratinocytes from (++) and (−/−) were cultured in the presence of the PPARβ/δ ligand GW0742 and/or GSK3787 at the indicated concentration as described in *Materials and Methods*. Quantitative real-time PCR was performed using total RNA isolated from cells to quantify mRNA expression of the PPARβ/δ target gene *Angptl4*. Values are the average normalized fold change as compared to vehicle control and represent the mean ± S.E.M. N = 3 biological replicates. Values with different letters are significantly different, $P \leq 0.05$, as determined by ANOVA and Bonferroni's multiple comparison test.

Fig. 4. GSK3787 antagonizes ligand-induced changes in PPARβ/δ-dependent gene expression in some, but not all, human cancer cell lines. Human cancer cell lines were cultured in the presence of the PPARβ/δ ligand GW0742 and/or GSK3787 at the indicated concentration as described in *Materials and Methods*. Quantitative real-time PCR was performed using total RNA isolated from cells to quantify mRNA expression of the PPARβ/δ target gene *ANGPTL4* or *ADRP*. Values are the average normalized fold change as compared to vehicle control and represent the mean ± S.E.M. N = 3 biological replicates. Values with different letters are significantly different, $P \leq 0.05$, as determined by ANOVA and Bonferroni's multiple comparison test.

MOL #65508

Fig. 5. GSK3787 antagonizes ligand induced reporter activity modulated by PPAR β/δ but also has weak agonist and antagonist activity for PPAR γ . NIH-3T3 cells were transiently transfected with reporter vectors to measure PPAR α , PPAR β/δ or PPAR γ -dependent activity as described in *Materials and Methods*. Cells were cultured for 24 h in the presence of 0.3 μ M GW7647, 0.3 μ M GW501516, 0.3 μ M GW1929 and/or 1.0 μ M GSK3787 before analysis of reporter activity. Values represent the average of independent triplicate samples \pm S.D.. N = 3 biological replicates. Mean values for each PPAR reporter assay with different letters are significantly different, $P \leq 0.05$, as determined by ANOVA and Bonferroni's multiple comparison test.

Fig. 6. GSK3787 antagonizes ligand induced recruitment of co-activator peptides and dissociation of co-repressor peptides from the LBD of PPAR β/δ in vitro. Interaction of fluorescein-labeled co-activator or co-repressor peptide and recombinant GST-PPAR β/δ bound by a terbium-labeled anti-GST antibody was determined by TR-FRET. (A) Interaction of the co-repressor peptide SMRT ID2 with the LBD of PPAR β/δ in the absence of ligand (GW501516). (B) Interaction of the co-repressor peptide SMRT ID2 with the LBD of PPAR β/δ in the presence of ligand (0.15 μ M GW501516). (C) Interaction of the co-activator peptide C33 with the LBD of PPAR β/δ in the absence of ligand (GW501516). (D) Interaction of the co-activator peptide C33 with the LBD of PPAR β/δ in the presence of ligand (0.15 μ M GW501516). Results are expressed as the ratio of fluorescence intensity at 520 nm (fluorescein emission excited by terbium

MOL #65508

emission) and 495 nm (terbium emission). Values represent the average of independent triplicate samples \pm S.D.. N = 3 biological replicates. *significantly different from control, $P \leq 0.05$, as determined by ANOVA and Bonferroni's multiple comparison test.

Fig. 7. GSK3787 antagonizes ligand induced recruitment of co-activator peptides and dissociation of co-repressor peptides from the LBD of PPAR β/δ and PPAR γ in vitro. Interaction of fluorescein-labeled co-activator or co-repressor peptide and recombinant GST-PPAR γ bound by a terbium-labeled anti-GST antibody was determined by TR-FRET. (A) Interaction of the co-activator peptide TRAP220 and the co-repressor peptides SMRT ID2 and NCoR ID2 with the LBD of PPAR β/δ in the absence of ligand (GW501516). (B) Interaction of the co-activator peptide TRAP220 and the co-repressor peptides SMRT ID2 and NCoR ID2 with the LBD of PPAR γ in the absence of ligand (GW1929) (C) Interaction of the co-activator peptide TRAP220 and the co-repressor peptide SMRT ID2 with the LBD of PPAR β/δ in the presence of ligand (0.15 μ M GW501516). (D) Interaction of the co-activator peptide TRAP220 and the co-repressor peptide SMRT ID2 with the LBD of PPAR γ in the presence of ligand (0.5 μ M GW1929). Results are expressed as the ratio of fluorescence intensity at 520 nm (fluorescein emission excited by terbium emission) and 495 nm (terbium emission). Values represent the average of independent triplicate samples \pm S.D.. N = 3 biological replicates. *significantly different from control, $P \leq 0.05$, as determined by ANOVA and Bonferroni's multiple comparison test.

MOL #65508

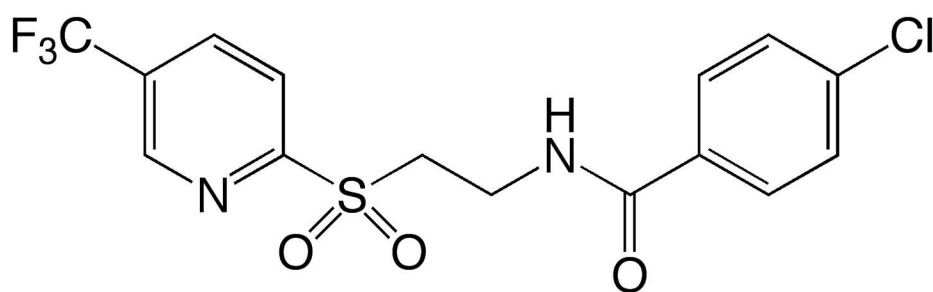
Fig. 8. Effect of GSK3787 on expression of a PPAR γ target gene and adipocyte differentiation. NIH 3T3-L1 cells were differentiated into adipocytes and then cultured in the presence of rosiglitazone, GSK3787 or rosiglitazone and GSK3787 as described in *Materials and Methods*. (A, B) Expression of *ap2* mRNA was quantified by qPCR. Values are the average normalized fold change as compared to vehicle control and represent the mean \pm S.E.M. (C) Cells were stained with Oil Red O and relative staining intensity quantified by measuring absorbance at 570 nm as described in *Materials and Methods*. Values represent the mean \pm S.E.M.. N = 3 biological replicates. Values with different letters are significantly different, $P \leq 0.05$, as determined by ANOVA and Bonferroni's multiple comparison test.

Fig. 9. Effect of GSK3787 on glucose tolerance. Wild-type () or *Ppar β/δ* -null (—/—) mice were treated with GW0742 (10 mg/kg), GSK3787 (10 mg/kg), or rosiglitazone (20 mg/kg) as described in *Materials and Methods*. Glucose tolerance tests were performed to determine the effect of PPAR β/δ agonism, PPAR β/δ antagonism and PPAR γ agonism on glucose tolerance in wild-type (*Ppar β/δ*) or *Ppar β/δ* -null (*Ppar β/δ ^{-/-}*) mice. N = 3 biological replicates. The P values for the areas under the curve for GW0742-, rosiglitazone-, or GSK3787-treated wild-type mice are 0.03, 0.07, 0.076 and the P values for GW0742-, rosiglitazone-, or GSK3787-treated *Ppar β/δ* -null mice are 0.90, 0.08, 0.87.

Table 1. Doubling times (hours) for human cancer cell lines following treatment with either a PPAR β/δ agonist (GW0742) or antagonist (GSK3787). Doubling times were calculated during the exponential growth phase as described in *Materials and Methods*. Values represent the mean \pm S.E.M.. Values with different superscript letters within a column are significantly different at $P \leq 0.05$.

Treatment	MCF7	Huh7	HepG2	A431	A549	H1838
DMSO	9.2 \pm 0.2 ^a	18.5 \pm 0.6 ^a	23.5 \pm 1.0 ^a	22.8 \pm 1.0 ^a	14.8 \pm 0.3 ^a	8.8 \pm 0.2 ^a
0.1 μ M GW0742	8.4 \pm 0.1 ^a	17.1 \pm 0.4 ^a	22.8 \pm 0.6 ^a	22.0 \pm 0.3 ^a	15.9 \pm 0.2 ^a	8.9 \pm 0.3 ^a
1.0 μ M GW0742	8.5 \pm 0.1 ^a	19.0 \pm 0.2 ^a	22.8 \pm 0.4 ^a	22.5 \pm 0.9 ^a	15.1 \pm 0.3 ^a	8.4 \pm 0.3 ^a
10 μ M GW0742	8.6 \pm 0.1 ^a	16.5 \pm 0.6 ^a	22.9 \pm 0.8 ^a	22.0 \pm 0.8 ^a	15.6 \pm 0.3 ^a	9.0 \pm 0.2 ^a
DMSO	6.9 \pm 0.1 ^a	19.0 \pm 0.5 ^a	23.6 \pm 1.2 ^a	21.5 \pm 1.0 ^a	15.4 \pm 0.3 ^a	9.0 \pm 0.4 ^a
0.1 μ M GSK3787	6.8 \pm 0.1 ^a	18.9 \pm 0.4 ^a	21.9 \pm 0.5 ^a	20.7 \pm 0.8 ^a	14.9 \pm 0.3 ^a	8.4 \pm 0.3 ^a
1.0 μ M GSK3787	6.7 \pm 0.1 ^a	18.7 \pm 0.4 ^a	23.4 \pm 1.1 ^a	22.1 \pm 1.0 ^a	14.8 \pm 0.3 ^a	8.1 \pm 0.4 ^a
10 μ M GSK3787	6.6 \pm 0.1 ^a	18.8 \pm 0.4 ^a	22.1 \pm 0.5 ^a	24.6 \pm 1.8 ^a	15.1 \pm 0.3 ^a	7.8 \pm 0.4 ^a

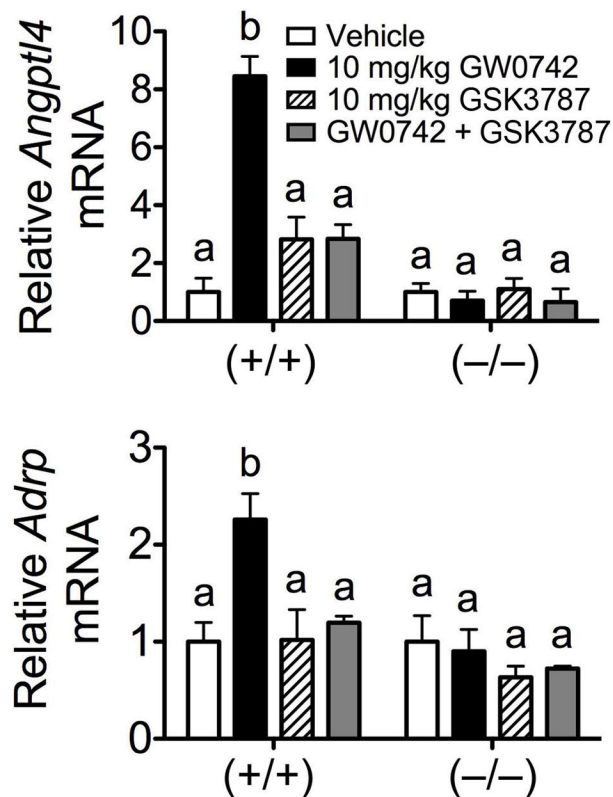
Fig. 1



GSK3787

Fig. 2

A.



B.

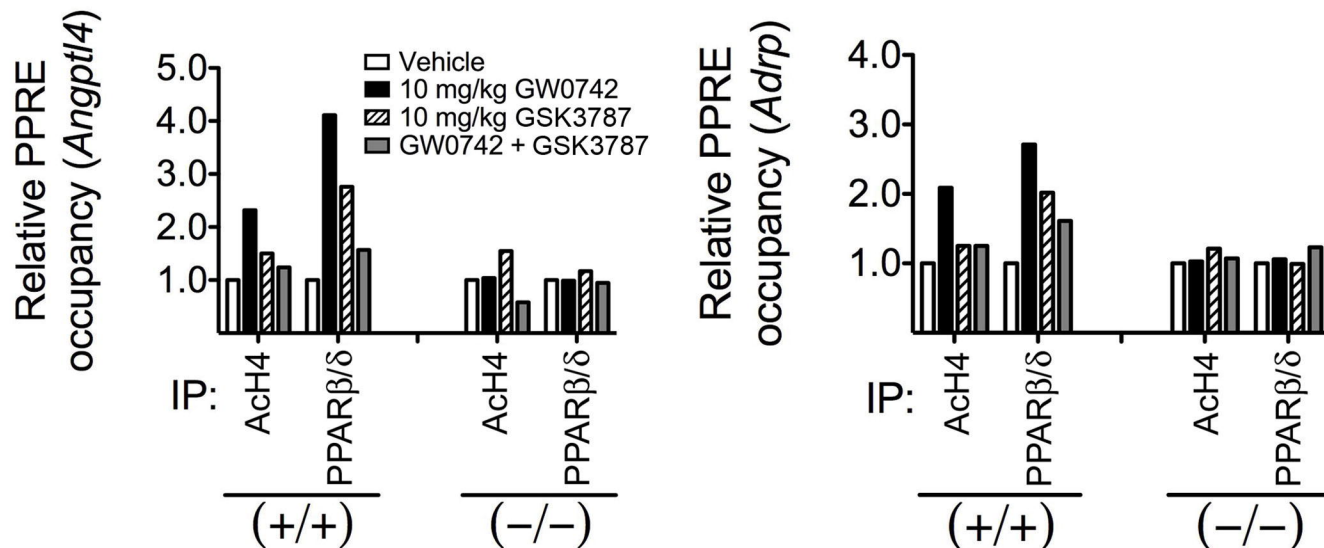


Fig. 3

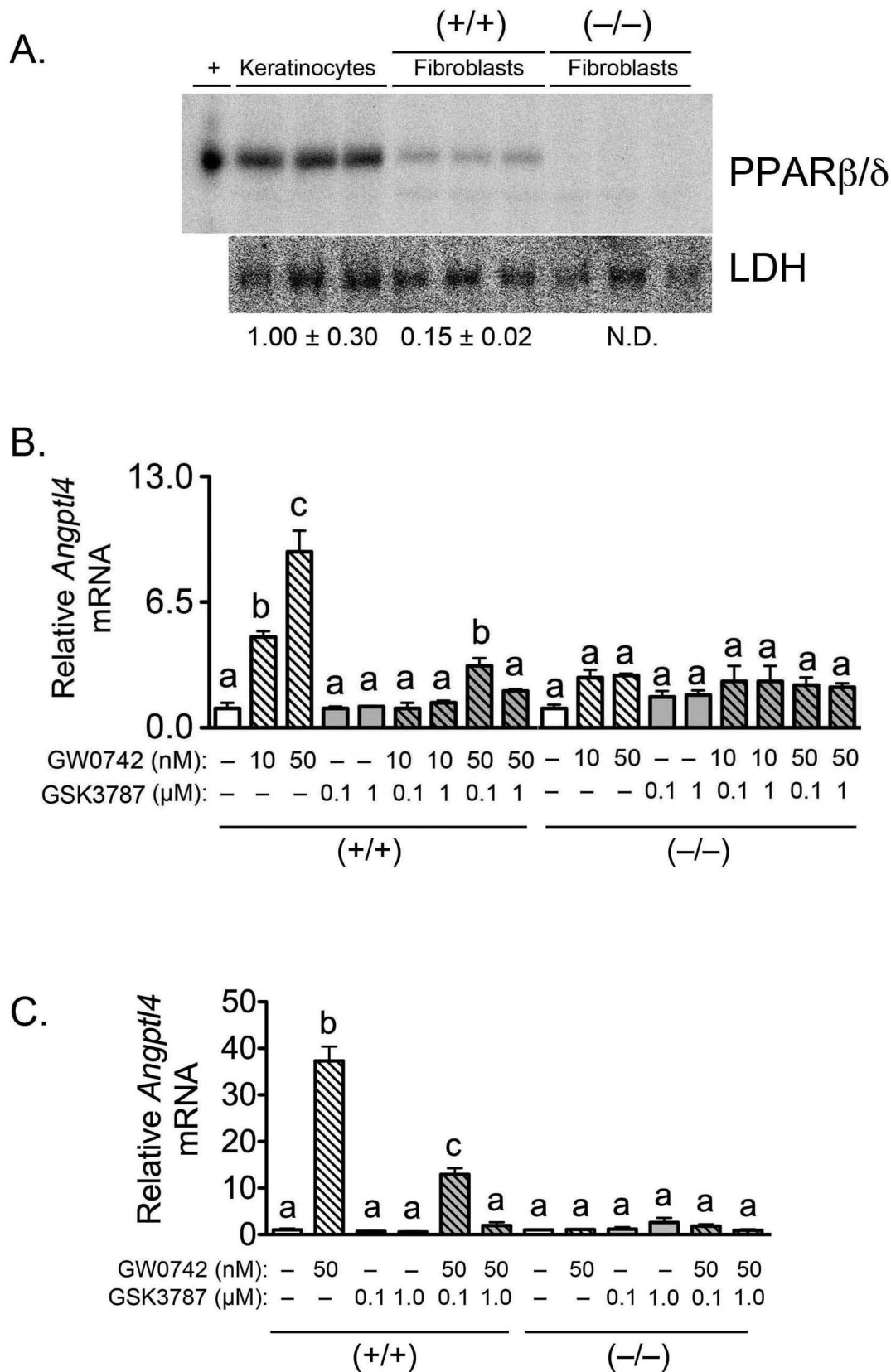


Fig. 4

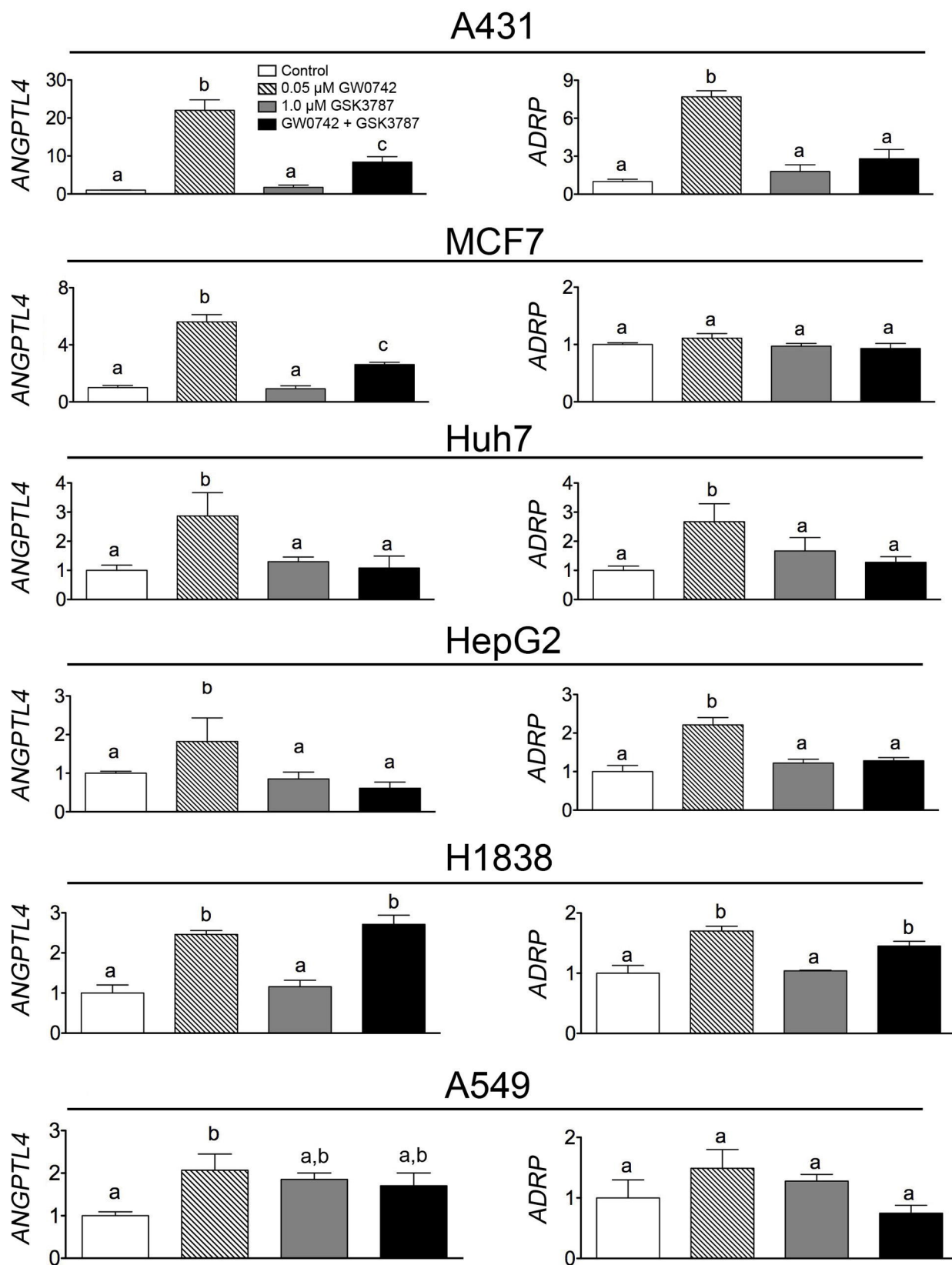


Fig. 5

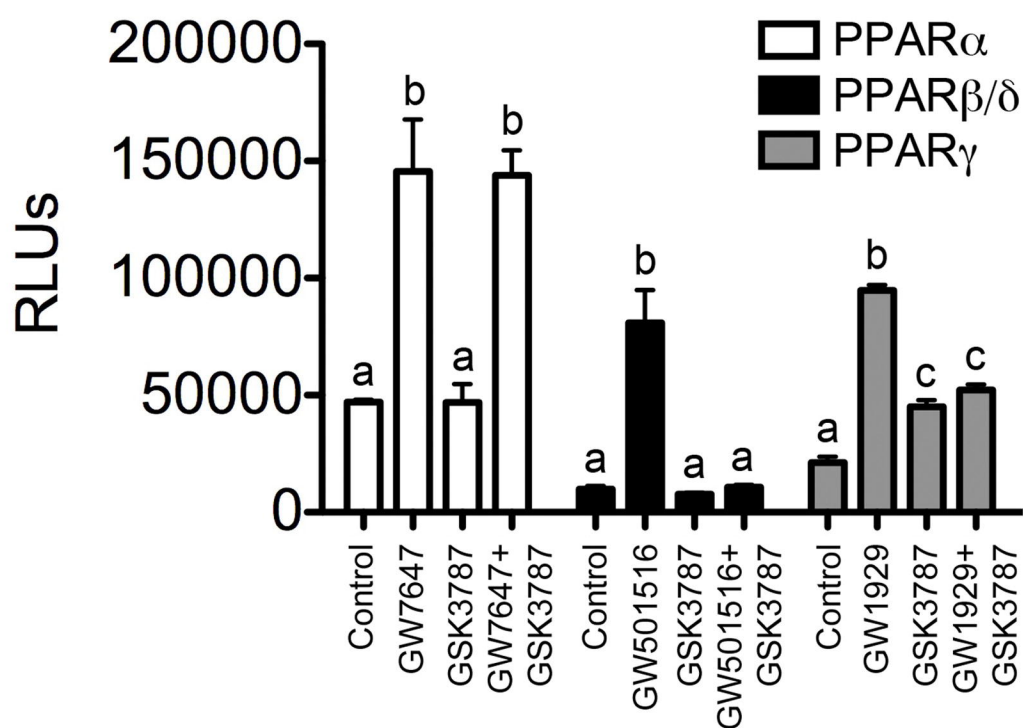


Fig. 6

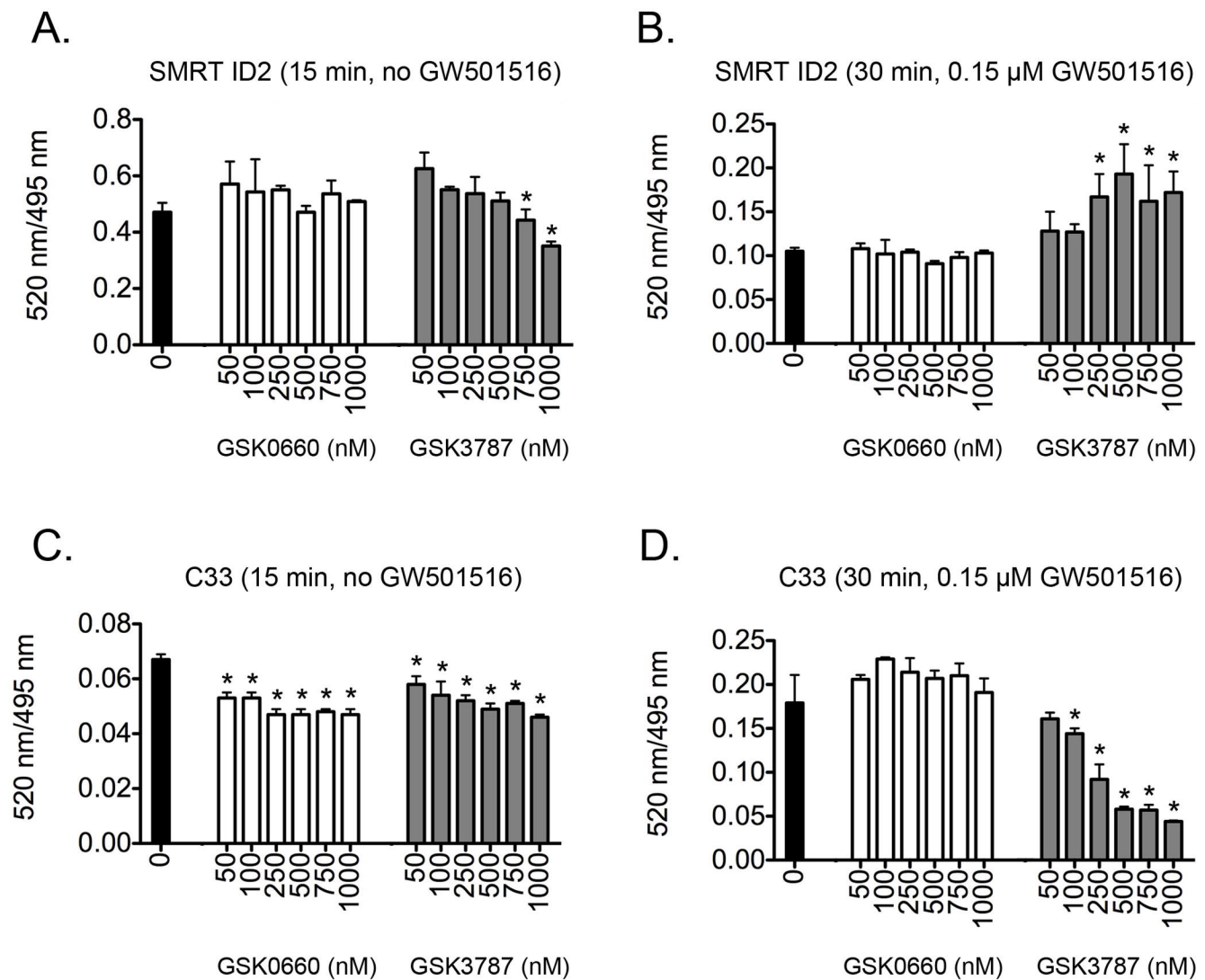


Fig. 7

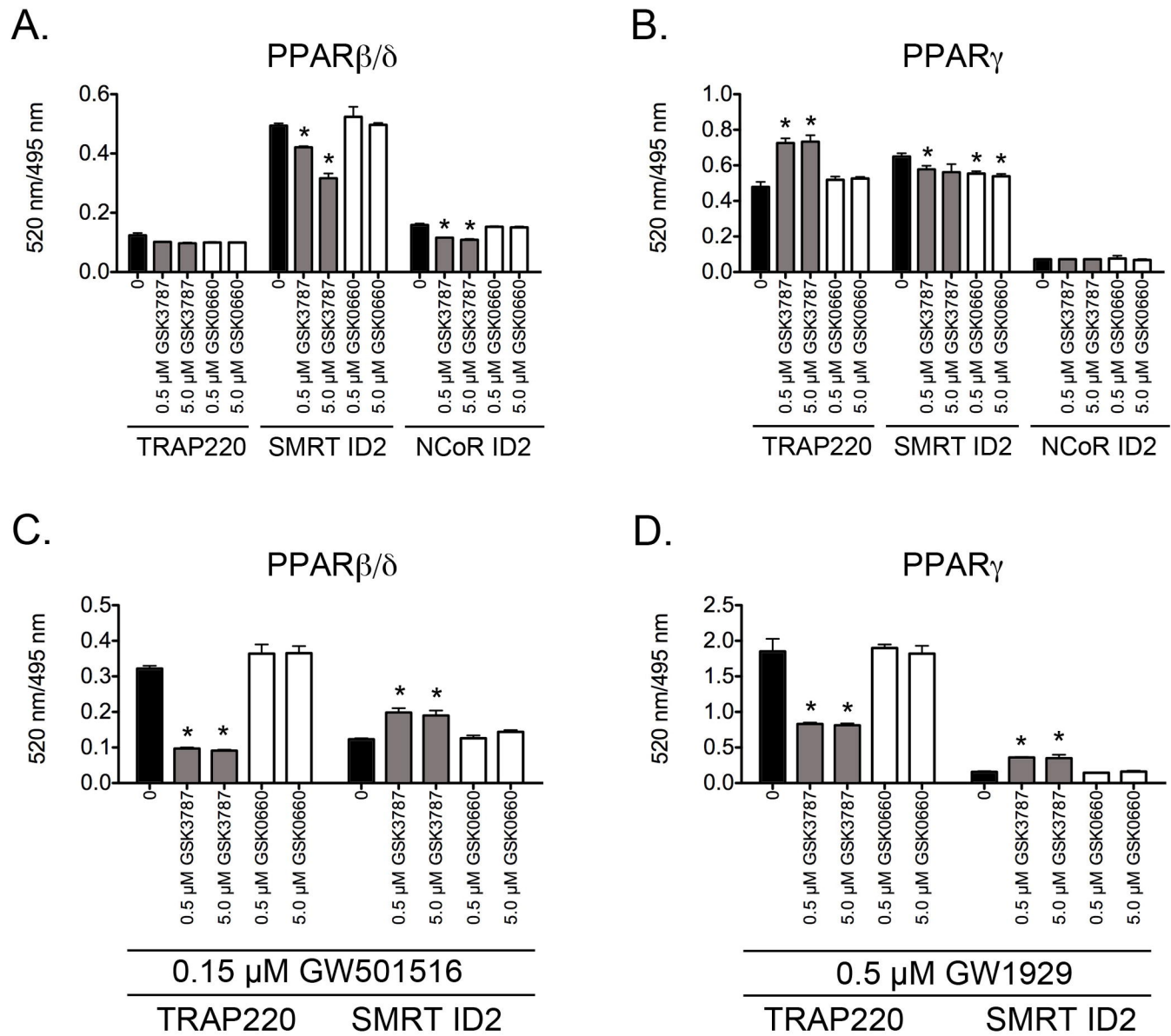


Fig. 8

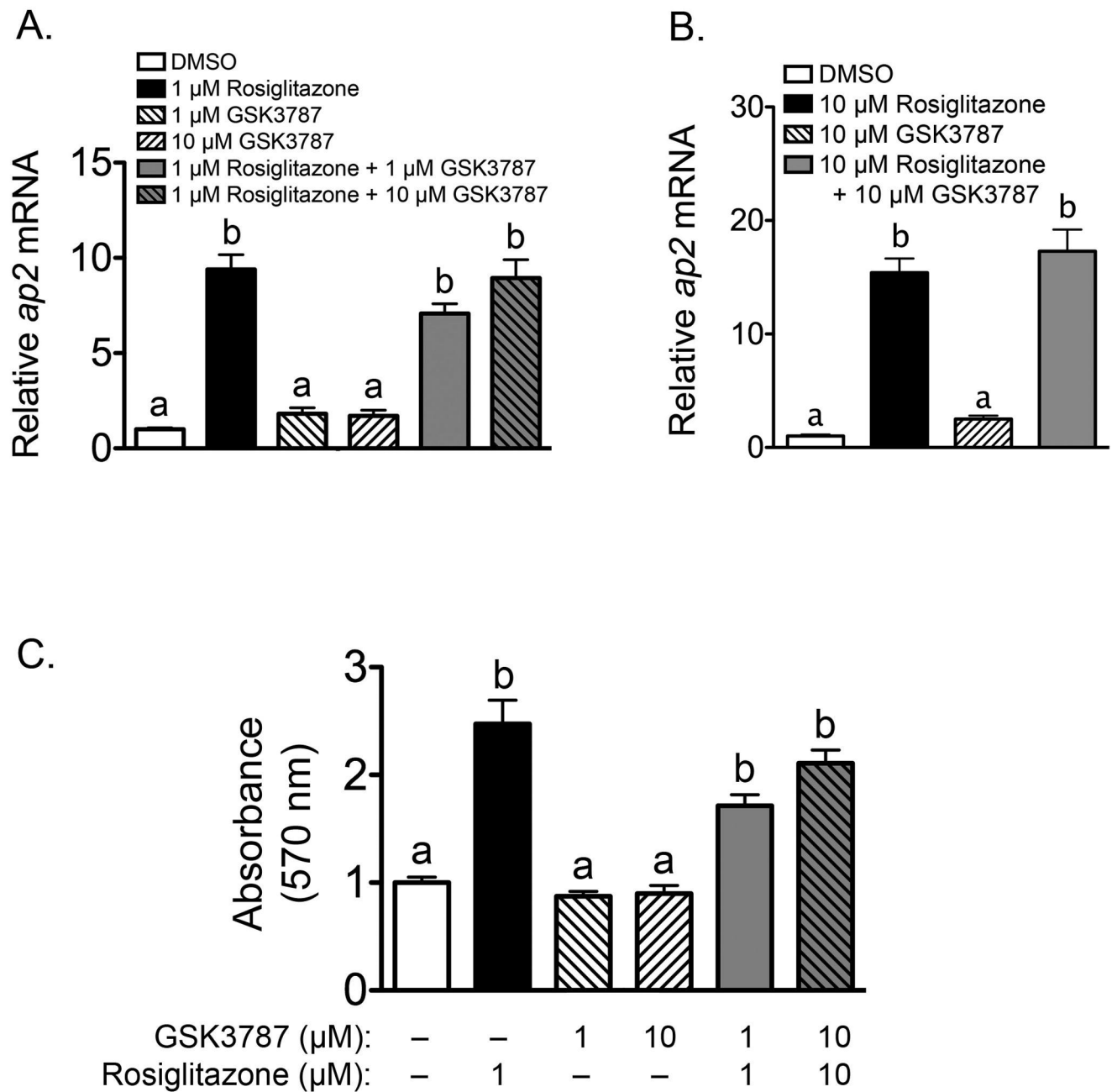


Fig. 9

